2013

Current-Based Fault Detection for Wind Turbine Systems via Hilbert-Huang Transform

Dingguo Lu
University of Nebraska-Lincoln, stan1860@huskers.unl.edu

Wei Qiao
University of Nebraska-Lincoln, wqiao@engr.unl.edu

Xiang Gong
University of Nebraska–Lincoln, xiang.gong@huskers.unl.edu

Liyan Qu
University of Nebraska-Lincoln, lqu2@unl.edu

Published in IEEE Power and Energy Society General Meeting (PES), 2013; doi:10.1109/PESMG.2013.6672999

Current-Based Fault Detection for Wind Turbine Systems via Hilbert-Huang Transform

Dingguo Lu, *Student Member, IEEE*, Wei Qiao, *Member, IEEE,* Xiang Gong, *Student Member, IEEE*, and Liyan Qu, *Member, IEEE*

***Abstract*—Mechanical failures of wind turbines represent a significant cost in both repairs and downtime. Detecting incipient faults of wind turbine components permits maintenance to be scheduled and failed parts to be repaired or replaced before causing failures of other components or catastrophic failure of the system. This paper proposes a Hilbert-Huang transform (HHT)-based algorithm to effectively extract fault signatures in generator current signals for wind turbine fault diagnosis by using the HHT's capability of accurately representing the instantaneous amplitude and frequency of nonlinear and nonstationary signals. A phase-lock-loop (PLL) method is integrated to estimate wind turbine rotating speed, which is then used to facilitate the fault detection. The proposed method is validated by a real direct-drive wind turbine with different types of faults. The experimental results demonstrate that the proposed method is effective to detect various faults in wind turbine systems as well as to reveal the severities of the faults.**

***Index Terms*—Condition monitoring, current, fault detection, Hilbert-Huang transform (HHT), wind turbine.**

I. Introduction

THE continuously growing number of wind turbine systems has increased the need to maintain and repair the wind turbines as they age and begin to fail. The cost of maintaining wind turbines shares a significant proportion of the total operational costs, often accounting for 10-15% and 25-30% of the energy generation costs for onshore and offshore wind turbines, respectively [1]-[3]. A considerable percentage of the maintenance cost is caused by unexpected drivetrain failures. These malfunctions also result in extended downtime as both parts and heavy equipment must be transported to the sites, which are often in remote areas [4]. Condition monitoring and fault detection (CMFD) techniques have been applied to detect diverse faults in wind turbines while the faults are still in an incipient phase, allowing for less downtime, increased lifespan and decreased wind power cost [4]-[6].

Online CMFD techniques can be classified into several categories based on the measurements employed. These measurements include electrical quantities (voltage, current and power), vibration, acoustic emission, temperature, oil constituent, etc. [4]-[6] Among them, vibration-based techniques have been the conventionally main focus of wind turbine CMFD [6] and proved successful for wind turbine systems as well as other industrial applications [7], [8]. The current-based techniques are gaining more attention for their advantages over vibration-based techniques in terms of accessibility, cost, implementation, and reliability [9]-[11]. The costs and complexity involved in current-based CMFD techniques are significantly lower than many other methods because current sensing is already implemented on most wind turbines and thus no additional sensors are required.

Online CMFD generally involves some forms of signal processing. Conventionally, the fast Fourier transform (FFT) and the short–time Fourier transform (STFT) are well-established methods that have achieved certain success and are widely used in industries [12]. However, they fail to characterize the faults in wind turbines which usually run in variable-speed conditions. The discrete wavelet transform (DWT), which is a time-frequency analysis method, is capable of presenting the time-varying frequency components of nonstationary signals. It has been successfully used in vibration-based gearbox CMFD [8]. However, the DWT suffers from inevitable issues of low resolution, interference terms, border distortion, and energy leakage [7].

The HHT is a relatively new method for time-frequency analysis that is able to calculate the instantaneous amplitude and frequency of nonlinear and nonstationary signals [13]. Unlike wavelet transforms, the HHT is based on an adaptive algorithm. Therefore, no prior knowledge of the signal is required to perform the HHT [14]. As a differentiation-based method, there is no uncertainty principle limitation in the result as that in the convolution-based wavelet and Fourier transforms. The HHT has been found powerful and successful in condition monitoring of electric machines using vibration data [7], and in detection of rotor bar failures of induction machines using stator current data [15].

This work investigates the application of the HHT to detect mechanical failures in wind turbines using generator stator current signals. Successful utilization of stator currents represents a cost-effective, nonintrusive CMFD technique for retrofitting existing condition monitoring methods for wind turbines. The proposed method is testified for a real direct-drive wind turbine with blade imbalance, blade misalignment and bearing inner-race faults. The experimental results lucidly prove the effectiveness of the proposed HHT-based algorithm for CMFD of wind turbine systems.

This work was supported in part by the U.S. Department of Energy under Grant DE-EE0001366 and the Nebraska Center for Energy Sciences Research.

The authors are with the Department of Electrical Engineering, University of Nebraska-Lincoln, Lincoln, NE 68588-0511 USA (e-mail: stan1860@huskers.unl.edu; wqiao@engr.unl.edu; xiang.gong@huskers.unl.edu; lqu2@unl.edu).

II. Hilbert-Huang Transform-based CMFD Algorithm

The HHT was initially developed by Norden E. Huang to analyze the nonlinear and nonstationary nature complex waves [13]. The HHT integrates the Hilbert transform spectrum analysis with Empirical Model Decomposition (EMD) to produce an experience-based method for generating time-frequency spectra of a variety of nonlinear and nonstationary signals.

A. Empirical Mode Decomposition

In order to use the properties of the Hilbert transform to determine the instantaneous amplitude and frequency of a signal, the signal must meet the requirements of an Individual Model Function (IMF). An IMF can be defined as a class of functions satisfying the following conditions [13]:

1) In the whole dataset, the number of extrema and the number of zero-crossings must either equal or differ at most by one;
2) At any point, the mean value of the envelopes defined by the local maxima and minima is zero.

Using the definition of IMF, any signal can be decomposed into a set of IMFs. The EMD method is employed to obtain the IMFs of the signal by implementing a sifting process. The process starts by identifying all local extrema of the signal, and then a cubic spline is used to connect all the local maxima, which is define as the upper envelope. A similar process is then executed to generate a spline connecting the local minima to create the lower envelope. The upper and lower envelopes should contain all points in the original signal $x(t)$.

The mean value of the two envelopes is denoted as m_1, and the difference between the original signal $x(t)$ and m_1 is defined as h_1,

$$h_1(t) = x(t) - m_1(t) \tag{1}$$

The sifting operation in (1) yield h_1 from $x(t)$. Normally h_1 will not yet satisfy the requirements of an IMF after the first round of sifting [13]. Therefore, the process is repeated using h_1 as the original data and the result is h_{11},

$$h_{11}(t) = h_1(t) - m_{11}(t) \tag{2}$$

where m_{11} the mean value of upper and lower envelops in h_1. After repeating the process k times, h_{1k} will satisfy the requirements of an IMF,

$$h_{1k}(t) = h_{1(k-1)}(t) - m_{1k}(t) \tag{3}$$

The resulting time series is redefined as the first IMF, or designated as $c_1(t) = h_{1k}(t)$.

Checking must be performed on whether the number of zero crossings equals the number of extrema after each sifting step. A point where further sifting will no longer result in significant changes to the signal usually determines the stopping criterion for the sifting process. After the first IMF is found, it must be subtracted from the original data so the difference can be further sifted to generate other IMFs. This new signal, called r_1, is the residue of the original signal with c_1 removed,

$$r_1(t) = x(t) - c_1(t) \tag{4}$$

If the original data contains more than one IMF, the same sifting procedure as for $x(t)$ can be applied to the residue r_1. This process is repeated for each subsequent residue until the residue becomes a monotonic function from which no further IMFs can be extracted. The final set of IMFs and the last residue will contain all the components of the original signal such that

$$x(t) = \sum_{i=1}^{n} c_i(t) + r_n(t) \tag{5}$$

B. Hilbert Transform

Once the signal has been completely decomposed into a set of IMFs, the instantaneous amplitude and frequency of each IMF can be found by using the Hilbert transform. The Hilbert transform is used to find the complex conjugate $H[c_i(t)]$ for each of the real valued IMFs extracted from $x(t)$:

$$H[c_i(t)] = \frac{1}{\pi} PV \int_{-\infty}^{\infty} \frac{c_i(\tau)}{t-\tau} d\tau \tag{6}$$

where PV the principal value of the singular integral. With this definition, an analytic signal $Z_i(t)$ consisting of $c_i(t)$ and $H[c_i(t)]$ is formed as

$$Z_i(t) = c_i(t) + jH[c_i(t)] = a_i(t)exp[j\theta_i(t)] \tag{7}$$

where $a_i(t)$ and $\theta_i(t)$ the instantaneous amplitude and phase angle of the IMF, respectively. Both of them can be individually defined as

$$a_i(t) = \sqrt{c_i(t)^2 + \{H[c_i(t)]\}^2} \tag{8}$$

$$\theta_i(t) = arctan\left\{\frac{H[c_i(t)]}{c_i(t)}\right\} \tag{9}$$

Utilizing the instantaneous phase angle, the instantaneous frequency is then calculated as

$$\omega_i(t) = \frac{d\theta_i(t)}{dt} \tag{10}$$

Thus, the original signal can be expressed in (11),

$$x(t) = Re\left(\sum_{i=1}^{n} a_i(t)\exp\left[j\int \omega_i(t)dt\right]\right) \tag{11}$$

where the residue $r_n(t)$ has been left over; and $Re(\cdot)$ denotes the real part of a complex quantity.

By processing each IMF from the original signal as above, the full instantaneous frequency spectrum can be developed. Integrating the instantaneous amplitude and frequency calculated using the Hilbert transform, a time-frequency analysis of the signal can be accomplished.

C. Proposed HHT-Based CMFD Method

A novel algorithm is developed to employ the HHT for CMFD of a wind turbine system by using generator stator current measurements, as illustrated in Fig. 1. A PLL speed estimator is developed to estimate the shaft rotating speed of the wind turbine, which is then used for CMFD. The use of the shaft rotating speed signal simplifies the IMF extraction, as the PLL removes main harmonics from the current signal, and meanwhile increases the signal to noise ratio (SNR) of the signal to be processed [10], [11], [13].

After completing the steps to process the HHT for a fault at different severities, the results can be compared to identify the

severity of the fault. A process is developed to isolate and combine the amplitude of each IMF yielded by the HHT that falls within specific frequency ranges. Then the amplitude of the processed IMF around the frequencies of interest could then be averaged. By doing so, it is possible to create simple bar graphs comparing the average amplitudes of IMFs for the faulty wind turbine system against the healthy wind turbine. The results can be visually inspected to verify the presence of the fault in question as well as to identify its severity.

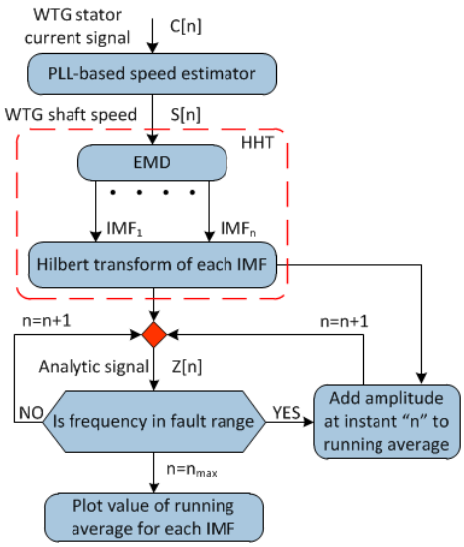

Fig. 1. Flowchart of the HHT-based fault detection algorithm.

The proposed algorithm innovatively explores the impacts of faults on stator current signatures, in the sense of variations in time domain over a frequency range, rather than the changes at a specific frequency or several specific frequencies. The latter is a commonly used approach to diagnose mechanical defects in wind turbine systems [11], [12], [16]. The proposed algorithm is especially useful for cases when no specific frequency components are available in the vibration/current measurements, or when the characteristic frequencies are nonstationary, and thus not directly observable.

III. Experimental Validation

A. Experimental System Setup

A 160-W Southwest Windpower Air Breeze wind turbine is deployed (Fig. 2) for experimental validation of the proposed HHT-based CMFD of wind turbine. The wind turbine is tested in an open-loop suction wind tunnel capable of providing stable and controllable wind speeds in the range of 0 to 10 m/s, and the wind turbine operates with a time-varying speed in a range of 6 to 13 Hz, accordingly. The nonstationary wind flow velocity inside the wind tunnel during experiments permits the wind turbine to operate in a situation similar to real-world conditions while still allowing for the control necessary to complete the experiments. One-phase stator current of the generator is measured via a Fluke current clamp, while the power generated by the wind turbine supplies a constant resistive load. The measurements are recorded through a National Instruments (NI) data acquisition system at a sampling rate of 10 kHz and the data are then stored by NI LabVIEW operating on a lab computer.

Blade and bearing faults constitute a considerable portion of all faults in wind turbine systems [17], [18]. A minor fault can cause significant consequences on the wind turbine systems. Due to wind turbines' delicate structure and high repairing costs, effective fault detection of blades and bearings is of significant interest to the wind industry. A variety of blade and bearing faults, happening in real applications, are duplicated in current experiments by pre-modifying the components, i.e., the blades and bearings.

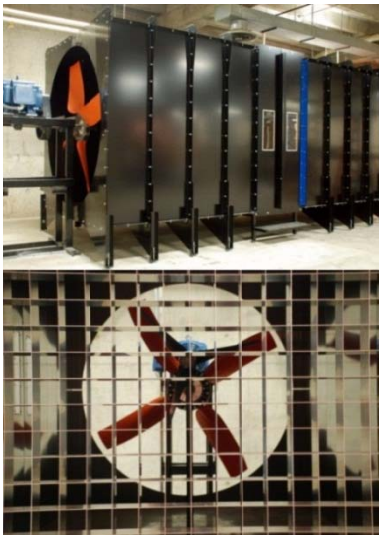

Fig. 2. Wind tunnel with a testing Air Breeze wind turbine.

B. Blade Imbalance

To create a blade imbalance fault, additional mass is added to or subtracted from the tip of one blade (Fig. 3). The mass is adjusted multiple times to emulate a blade imbalance of +1%, 2%, 3% and 5% off the original blade mass. Therefore, the experiments will represent five different levels of imbalance, including a baseline case where the three blades are balanced.

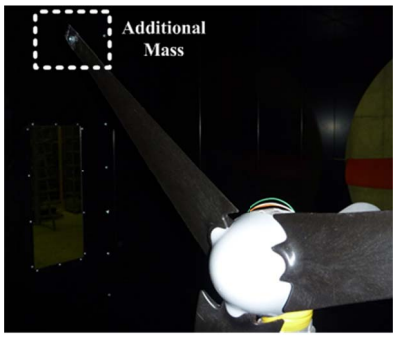

Fig. 3. Depiction of imbalance fault of a wind turbine blade.

The proposed method is applied to the generator stator current to obtain the IMFs of the wind turbine rotating speed, which is estimated by the PLL method. Based on the previous work using a 1P-invariant PSD method, it has already been

found that the imbalance fault introduces a change in the amplitude in the range of 6 to 13 Hz in the PSD spectrum of the shaft rotating speed estimated from the stator current [10]. Therefore, after extracting all the IMFs and calculating their respective amplitudes and frequencies, the second IMF is found to contain the majority of the 6 to 13 Hz frequency components (Fig. 4). The samples of the second IMF are then averaged in amplitude for each case, based on which a bar graph is generated in Fig. 5. From the comparison, a clear trend is evident that the average amplitude of the second IMF continuously increases because of the increasing severity of the fault. Therefore, the proposed method can not only identify but also quantify the level of blade imbalance of the wind turbine. The results corroborate with that obtained using the 1P-invariant PSD method in [10].

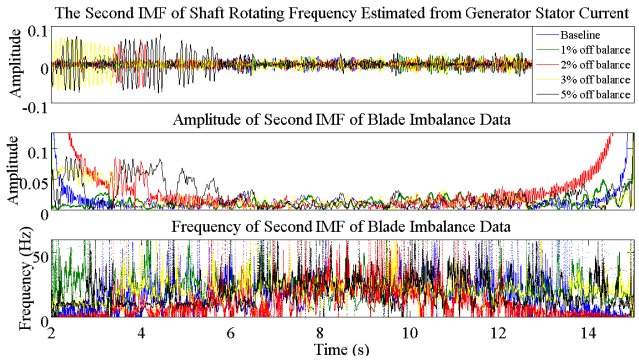

Fig. 4. Hilbert transform of the second IMF for blade imbalance case.

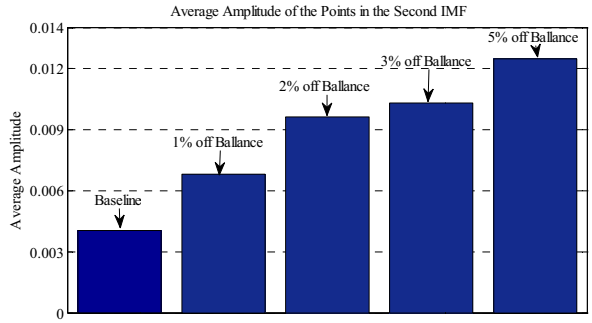

Fig. 5. Average amplitude of the second IMF for blade imbalance case.

C. Blade Misalignment

A blade misalignment is a blade that bends flapwise or edgewise, as illustrated in Fig. 6. A series of experiments are performed on edgewise bending blade to test the ability of the HHT-based method for detecting blade misalignment. To emulate the effect of blade edgewise bending, one blade of the testing turbine is affixed at 2, 4, and 6 degrees from its normal position, respectively. This effectively results in a blade imbalance with the drivetrain having larger mass in the direction towards which the blade is misaligned. Therefore, it is expected that the fault signatures of blade misalignment should be similar to that of the blade imbalance fault in previous subsection III-B.

Just as in the blade imbalance experiments, the second IMF is selected for the aforementioned reasons. A bar graph with the average amplitude of the IMF for each misalignment case is depicted in Fig. 7. A clear trend appears as the blade deviates from its normal position. The results are similar to those of blade imbalance, as discussed above that this phenomenon is expected due to the similarity between these two fault types.

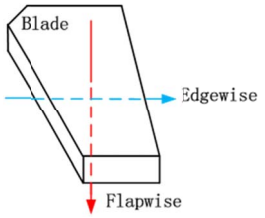

Fig. 6. Depiction of blade bending flapwise or edgewise.

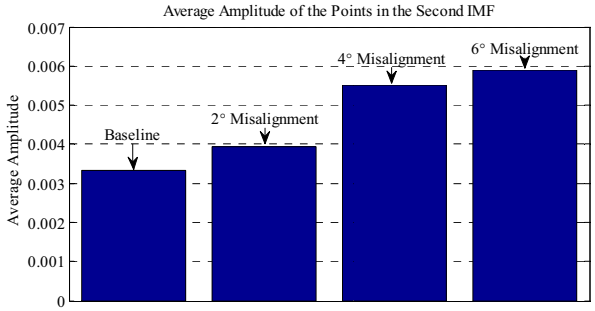

Fig. 7. Average amplitude of the second IMF for blade misalignment case.

D. Inner-Race Bearing Fault

The testing bearing used in the experiments is the main bearing of the Air Breeze wind turbine located between the rotors of the turbine and the generator (Fig. 8). An artificial hole is drilled in the inner race of a testing bearing to emulate an inner-race defect (Fig. 9). The damaged bearing is then switched with the wind turbine main bearing.

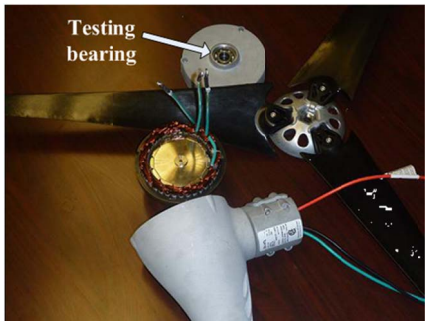

Fig. 8. Placement of the testing bearing in the Air Breeze wind turbine.

Fig. 9. Testing bearing with an inner-race fault.

Prior to processing the estimated shaft rotating speed for bearing fault detection, the estimated shaft speed for the

healthy bearing is concatenated with that for the faulty bearing. The purpose of agglutinating two sets of data under different conditions prior to the EMD is to make the results directly and visually comparable without a bar graph. This is because the IMF has no specified frequency range, the same signal components may end up in different IMFs. The results are split at the point where they were combined to produce two sets of results: one for the healthy bearing and the other for the faulty bearing. A significant difference exists in the third IMF, as indicated by Fig. 10. For the fault case, the amplitude of the third IMF dramatically increases, when compared to the baseline case. Therefore, the excitations of particular frequency components induced by the bearing inner-race fault can be successfully detected using the generator stator current via the proposed HHT-based method.

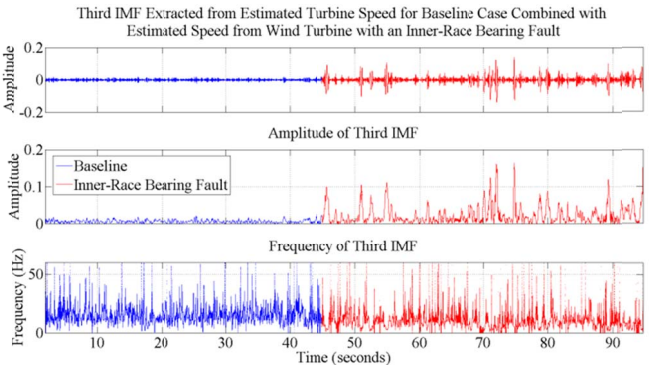

Fig. 10. Hilbert transform of the third IMF of the combined samples for bearing inner-race fault.

IV. Discussion & Conclusion

The HHT-based algorithm is capable of detecting mechanical faults based on time-frequency analysis. It can be directly applied to the nonlinear and nonstationary signals, without pre-processing to convert the characteristics frequencies to corresponding constant values. It overcomes the drawbacks of traditional frequency-based fault detection techniques that particular characteristic frequencies related to the faults should be pre-acquired. The HHT-based methods are believed to be non-frequency-based ones which require only a frequency range. Of course, using the frequency-based methods can be of great help in selection of the right IMFs that contain the objective frequency components.

An HHT-based technique has been proposed for online wind turbine CMFD using generator stator current measurements. The proposed method integrates a PLL to estimate the shaft rotating speed of the WTG from the measured stator current signal. The estimated shaft rotating speed is first processed by EMD method, which decomposes the signal into a set of IMFs. The Hilbert transform is then utilized to calculate the analytic signal for each IMF, from which the instantaneous amplitude and phase angle of each IMF can be derived and employed to generate fault signatures for wind turbine fault diagnosis.

The proposed method has been validated for the detection of various types of faults on wind turbine blade and main bearings. The experimental results have demonstrated that the proposed method has been successfully applied to the detection of blade imbalance, blade misalignment, as well as bearing inner-race fault. The successful applications of the proposed method using only the generator stator current signals can not only identify but also quantify the severity of the faults, representing a significant achievement in wind turbine CMFD.

V. References

[1] T. W. Verbruggen, "Wind Turbine Operation and Maintenance based on Condition Monitoring," Energy Research Center of the Netherlands, April, 2003.

[2] W. Musial and B. Ram, "Large-Scale Offshore Wind Power in the United States," National Renewable Energy Laboratory, September, 2010.

[3] E. J. Wiggelinkhuizen, T. W. Verbruggen, H. Braam, L. Rademakers, J. Xiang, S. Watson, G. Giebel, E. Norton, M. C. Tiplucia, A. MacLean, A. J. Christensen, E. Becker, and D. Scheffler, "CONMOW: Condition monitoring for offshore wind farms," in *Proc. 2007 European Wind Energy Conference and Exhibition*, Milan, Italy, 2007.

[4] B. Lu, Y. Li, X. Wu, and Z. Yang, "A review of recent advances in wind turbine condition monitoring and fault diagnosis," in *Proc. 2009 IEEE symposium on Power Electronics and Machines in Wind Applications*, Lincoln, NE, 2009, pp. 1-7.

[5] Z. Hameed, Y. S. Hong, Y. M. Cho, S. H. Ahn, and C. K. Song, "Condition monitoring and fault detection of wind turbines and related algorithms: A review," *Renewable and Sustainable Energy Reviews,* vol. 13, pp. 1-39, 2009.

[6] Y. Ding, E. Byon, C. Park, J. Tang, Y. Lu, and X. Wang, "Dynamic data-driven fault diagnosis of wind turbine systems," in *Proc. 7th International Conference on Computational Science, Part I*, Beijing, China, 2007.

[7] Z. K. Peng, P. W. Tse, and F. L. Chu, "An improved Hilbert–Huang transform and its application in vibration signal analysis," *Journal of Sound and Vibration,* vol. 286, pp. 187-205, 2005.

[8] N. Baydar and A. Ball, "Detection of gear failures via vibration and acoustic signals using wavelet transform," *Mechanical Systems and Signal Processing,* vol. 17, pp. 787-804, 2003.

[9] Y. Amirat, V. Choqueuse, M. E. H. Benbouzid, and J. F. Charpentier, "Bearing fault detection in DFIG-based wind turbines using the first intrinsic mode function," in *Proc. 2010 XIX International Conference on Electrical Machines*, Rome, Italy, 2010, pp. 1-6.

[10] X. Gong and W. Qiao, "Imbalance fault detection of direct-drive wind turbines using generator current signals," *IEEE Trans. Energy Conversion,* vol. 27, pp. 468-476, 2012.

[11] X. Gong and W. Qiao, "Bearing fault detection for direct-drive wind turbines via stator current spectrum analysis," in *Proc. 2011 IEEE Energy Conversion Congress and Exposition*, pp. 313-318.

[12] X. Gong and W. Qiao, "Current-based online bearing fault diagnosis for direct-drive wind turbines via spectrum analysis and impulse detection," in *Proc. 2012 IEEE Symposium on Power Electronics and Machines in Wind Applications*, 2012, pp. 1-6.

[13] N. E. Huang, *Hilbert-Huang Transform And Its Applications*. Singapore: World Scientific, 2005.

[14] J. A. Antonino-Daviu, M. Riera-Guasp, M. Pineda-Sanchez, and R. B. Perez, "A critical comparison between DWT and Hilbert-Huang-based methods for the diagnosis of rotor bar failures in induction machines," *IEEE Trans. Industry Applications,* vol. 45, pp. 1794-1803, 2009.

[15] Z. K. Peng and F. L. Chu, "Application of the wavelet transform in machine condition monitoring and fault diagnostics: A review with bibliography," *Mechanical Systems and Signal Processing,* vol. 18, pp. 199-221, 2004.

[16] D. Lu, X. Gong, and W. Qiao, "Current-based diagnosis for gear tooth breaks in wind turbine gearboxes," in *Proc. 2012 IEEE Energy Conversion Congress & Exposition*, pp. 3780-3786.

[17] Y. Amirat, M. E. H. Benbouzid, E. Al-Ahmar, B. Bensaker, and S. Turri, "A brief status on condition monitoring and fault diagnosis in wind energy conversion systems," *Renewable and Sustainable Energy Reviews,* vol. 13, pp. 2629-2636, July 15 2009.